Available online at www.sciencedirect.com
SCIENCE DIRECT®
Physics Letters A 325 (2004) 70–78
PHYSICS LETTERS A
www.elsevier.com/locate/pla

Influence of the coupling between the normal and lateral motions on surface states of a semi-infinite superlattice with a cap layer

Wei-Qing Huang [a,b], Ke-Qiu Chen [a,*], Z. Shuai [a,*], Lingling Wang [b], Wangyu Hu [b]

[a] *Laboratory of Organic Solids, Center for Molecular Sciences, Institute of Chemistry, Chinese Academy of Sciences, 100080 Beijing, PR China*

[b] *Department of Applied Physics, Hunan University, 410082 Changsha, PR China*

Received 28 November 2003; accepted 11 March 2004

Communicated by J. Flouquet

Abstract

Using an effect-barrier height method, we investigate theoretically the influence of the coupling between normal and lateral motions of an electron on the surface electron states in a semi-infinite $Al_{0.3}Ga_{0.7}As/GaAs$ superlattice with a cap layer consisting of ternary mixed crystal $Al_xGa_{1-x}As$ within the framework of effective-mass theory. Previous works on the surface states in semi-infinite superlattice paid much less attention to the coupling effect. However, our study showed that the coupling effect cannot be neglected when the difference of the effective mass of the electron between the well and barrier layers exists. It is found that the existence and features of the surface electron states, especially the higher-lying surface electron states, as well as the energy positions and widths of the miniband and minigaps are sensitively dependent on the transverse wave number. A brief analysis of these results is given.

PACS: 73.20.-r; 73.20.Dx

1. Introduction

Rapid advances in epitaxial growth techniques make it possible to fabricate a variety of superlattices (SLs) such as periodic, quasiperiodic and random SLs from various kinds of materials including semiconductors, metals and magnetically ordered materials with well-controlled the thickness of each layer and compositions. These man-made structures have received considerable attention for many years owing to their novel physical properties, which can be tailored and controlled. It is well known that the energy spectrum of an ideal infinite SL is composed of minibands alternating with minigaps. The localized electron states exist possibly in the minigap if any deviations of the structure from strict periodicity appear by the existence of inhomogeneities such as a surface [1–6], structural defect [7–9]. Similar phenomena can also be found in acoustic [10,11] and optical vibrations [12–14] in such structures. Surface electron states should be considered when we design heterostrucutre devices, since surface is a necessity in reality. The properties of the

* Corresponding authors.
E-mail addresses: keqiuchen@iccas.ac.cn (K.-Q. Chen), zgshuai@iccas.ac.cn (Z. Shuai).

0375-9601/$ – see front matter
doi:10.1016/j.physleta.2004.03.022

surface electron states in SLs have been extensively investigated both experimentally [4–6,15] and theoretically [16–24] during the past two decades. By terminating a GaAs/$Ga_{1-x}Al_xAs$ SL with an AlAs (or $Al_{0.15}Ga_{0.85}As$) layer, Ohno et al. have made the first observation of electronic states localized at an internal surface by using a combination of photoluminescence (PL), photoluminescence excitation (PLE) and photocurrent (PC) spectroscopies, and calculated the energies of the surface electron states and the extended states for nine wells according to the envelope function approximation (EFA) [5,6]. The effect of the SL surface on the electronic properties was studied by modifying the bulk parameters and keeping the surface parameters fixed [16,20,24], or by changing the height of the substrate barrier and the SL parameters [17,22,23]. The surface electron states in the presence of the cap layer [25] or electric field [18] were also reported. More recently, a comprehensive review of the localized electron states in SLs, in particular, surface electron states, occurring at the terminating-barrier/superlattice interface was given by Stęślicka et al. [26]. To date, previous works on surface states based upon the effective mass parabolic conduction-band model paid much less attention to the coupling effect between normal and lateral motions of an electron. However, recently studies have showed that the coupling effect due to the mismatch of electron effective mass in different thin layers lead to the significant dependence of the transmission probability on the transverse wave vector k_{xy} in single barrier [27] and multibarrier [7,28] structures at zero magnetic field, and in a infinite SL with structural defect at finite magnetic field [9].

In the present Letter, we investigated the effect of the coupling between the normal and lateral motion on surface states in a semi-infinite SL with a cap layer by adopting an effect-barrier height method. A comparisons of surface electron levels between neglecting and including this effect is made. Our results show that the existence and features of the surface electron states dramatically depend on the transverse wave number and cap layer.

This Letter is organized as follows: in the next section gives a brief description of the theoretical framework of our calculation. The numerical results are presented in the Section 3 with analyzes, and a brief summarization is made in the last section.

2. Model and formalism

We consider a structure as schematically depicted in Fig. 1, in which a cap layer labelled as d (material $Al_xGa_{1-x}As$) with a thickness of W_d is embedded between a semi-infinite SL with the unit cell composed of a (GaAs) and b ($Al_{0.3}Ga_{0.7}As$) materials and a semi-infinite homogeneous substrate ($Al_yGa_{1-y}As$) labelled as c. The potential heights of the materials a, b, c and d are U_a, U_b, U_c and U_d, respectively. The thicknesses of the constituent layers a and b are W_a and W_b, respectively, and the period of the semi-infinite superlattice is $W = W_a + W_b$. We choose the growth direction of the SL as the z-axis.

To obtain the surface states, one has to solve the Schrödinger equation

$$\left[-\frac{\hbar^2}{2m}\frac{d^2}{dz^2} + U(z)\right]\phi(z) = E\phi(z), \tag{1}$$

where m is the electron effective mass, $U(z)$ is the potential height function, and E the eigenenergy of the surface state. The potential height is defined as $U(z) = U_a = 0$ (in the a layer) and $U(z) = U_\beta$ (in the β ($\beta = b, c, d$) layer), with U_β is the offset of the conduction band edge between β and a layer.

Within the envelope function effective-mass approximation, the 1D Schrödinger equation satisfied by the longitudinal envelope-wave function $\phi(z)$ is described by

$$-\frac{\hbar^2}{2}\frac{d}{dz}\frac{1}{m(z)}\frac{d}{dz}\phi(z) + U(z)\phi(z) = \left[E - \frac{\hbar^2 k_{xy}^2}{2m(z)}\right]\phi(z), \tag{2}$$

where k_{xy} is the transverse wave vector, and $U(z)$ and $m(z)$ the position-dependent potential and the effective mass. From Eq. (1), we have $E_z^\alpha = E - E_{xy}^\alpha$ ($\alpha = a, b, c, d$) representing the longitudinal energies of the electron in the α layer, where $E_{xy}^\alpha = \hbar^2 k_{xy}^2/2m_\alpha$ is the transverse kinetic energies in the α layer. Taken into account the difference of the effective mass of the electron in different layer in a period of the superlattice, i.e., $m_a \neq m_b$, both the transverse kinetic-energy and longitudinal energy components of the electron no longer keep their conservation individually. We introduce an effective barrier height

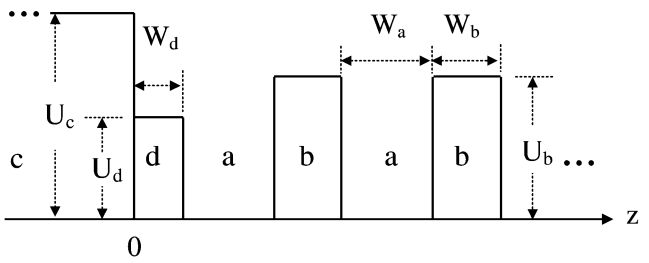

Fig. 1. Conduction-band profile of a semi-infinite superlattice with a cap layer d attached to semi-infinite homogeneous medium c. W_d, W_a and W_b denote the thickness of the cap layer and the two constituent layers of the unit cell of the semi-infinite SL, respectively. U_c, U_d and U_b denote the potential height of the substrate, the cap layer, and the barrier layer of the SL, respectively.

as

$$U_\beta(k_{xy}) = U_\beta - \left(1 - \frac{m_a}{m_\beta}\right)\frac{\hbar^2 k_{xy}^2}{2m_a}, \tag{3}$$

where U_β is the potential height of the β layer.

Eq. (1) can then be rewritten as

$$-\frac{\hbar^2}{2}\frac{d}{dz}\frac{1}{m(z)}\frac{d}{dz}\phi(z) + U_{\text{eff}}(z)\phi(z) = E_z\phi(z), \tag{4}$$

where $E_z \equiv E_z^a = E - (\hbar^2 k_{xy}^2/2m_a)$, and the effective potential $U_{\text{eff}}(z)$ is defined as follows

$$U_{\text{eff}}(z) = \begin{cases} 0 & \text{in the } a \text{ layer,} \\ U_\beta(k_{xy}) & \text{in the } \beta \text{ layer.} \end{cases} \tag{5}$$

From Eq. (4), it is evident that the longitudinal component of the motion of the electron is dependent on the transverse wave vector k_{xy} when taking into account the difference of the effective mass of the electron in the different layers.

We now applying Eqs. (4), (5) to investigate localized electron levels in the structure as shown in Fig. 1. The longitudinal envelope-wave function for the slab of material a in the region $nW < z < nW + W_a$ can be written as

$$\phi(z) = e^{iq_z(n-1)W}\left[A_a e^{ik_a(z-z_a^n-W_d)} + B_a e^{-ik_a(z-z_a^n-W_d)}\right]. \tag{6}$$

While for slab b in the region $nW + W_a < z < (n+1)W$, we have

$$\phi(z) = e^{iq_z(n-1)W}\left[A_b e^{ik_b(z-z_b^n-W_d-W_a)} + B_b e^{-ik_b(z-z_b^n-W_d-W_a)}\right], \tag{7}$$

where z_a^n and z_b^n is the center coordinate of the a and b layers in the nth ($n = 1, 2, 3, \ldots$) period of the SL, W is the period of the SL, and q_z is the attenuation constant and its imaginary part should be positive for the localized surface states. In the region $0 < z < W_d$ we have

$$\phi(z) = A_d e^{ik_d(z-z_d)} + B_d e^{-ik_d(z-z_d)}, \tag{8}$$

where z_d represents the center coordinate of the d layer. And in the region $z < 0$ the wave function decays exponentially as

$$\phi(z) = A_c e^{k_c z}, \tag{9}$$

where the longitudinal wave number of the electron is given by

$$k_\mu = \left[\frac{2m_\mu(E_z - U_{\mu,\text{eff}})}{\hbar^2}\right]^{1/2} \quad (\mu = a, b, d), \tag{10}$$

and

$$k_c = \left[\frac{2m_c(U_{c,\text{eff}} - E_z)}{\hbar^2}\right]^{1/2}. \tag{11}$$

Note that k_c is real and positive, i.e., $E_z < U_{c,\text{eff}}$. For localized electron states lying within minigaps, the Bloch wave number q_z should take a complex values in the form as

$$q_z = \frac{n\pi}{W} + iq \quad (q > 0, n = 1, 2, \ldots). \tag{12}$$

n denotes the index of minigaps. It is worth pointing out that the imaginary Bloch wave number q (decay factor) reflects the localization degree of the localized modes in the vicinity of the cap layer.

By imposing the boundary conditions at interfaces: $\phi(z)$ and $\phi'(z)/m(z)$ should be continuous at each

interface, we can obtain the following equations

$$\cos(q_z W) - \frac{1}{2}(\hat{P}_{11} + \hat{P}_{22}) = 0, \tag{13}$$

$$(F_{cd}+1)\left(\hat{S}_{21} + \hat{S}_{22}\frac{e^{-iq_z W} - \hat{P}_{11}}{\hat{P}_{12}}\right) - (F_{cd}-1)\left(\hat{S}_{11} + \hat{S}_{12}\frac{e^{-iq_z W} - \hat{P}_{11}}{\hat{P}_{12}}\right)e^{-ik_d W_d} = 0, \tag{14}$$

where

$$F_{cd} = \frac{ik_d m_c}{m_d k_c}, \tag{15}$$

$$\hat{S} = \hat{T}^{-1}(m_d, k_d, W_d)\hat{T}(m_a, k_a, -W_a), \tag{16}$$

$$\hat{P} = \hat{T}^{-1}(m_a, k_a, W_a)\hat{M}(m_b, k_b, W_b) \times \hat{T}(m_a, k_a, -W_a), \tag{17}$$

with

$$\hat{M}(m, k, z) = \hat{T}(m, k, -z)\hat{T}^{-1}(m, k, z), \tag{18}$$

and

$$\hat{T}(m, k, z) = \begin{pmatrix} e^{ikz/2} & e^{-ikz/2} \\ (ik/m)e^{ikz/2} & (-ik/m)e^{ikz/2} \end{pmatrix}. \tag{19}$$

Eqs. (13), (14) determine the localized electron states lying within the minigaps. For real Bloch wave number q_z, Eq. (13) gives the dispersion relation of the electronic states in SL. Here, it should be particularly noted that in numerical studies of the dispersion relations of the surface electron states one seeks the roots of Eq. (14). Once a root is found, it is necessary to insure that the imaginary part of the attenuation constant q_z determined by equation (13) is positive (namely $(q_z) > 0$) for the surface electron states. In the following section, we present the results of numerical calculations of the dispersion relation of the surface states for the structure shown in Fig. 1. In the calculations, we employ those values of the potential function and the effective-mass values of $Al_xGa_{1-x}As$: $U(x) = 944x$ meV and $m(x) = (0.067 + 0.083x)m_e$, m_e being the free-electron mass [4].

3. Numerical results and analyzes

We first take into account the influence of the transverse wave number k_{xy} on the longitudinal energy components of the surface electron states. The calculated surface electron structures are shown in Fig. 2 for different concentrations y of the semi-infinite homogeneous substrate c: (a)–(f) correspond to $y =$ 0.1, 0.15, 0.23, 0.4, 0.5 and 1.0, respectively. Here, we take $W_a = 4.0$ nm, $W_b = 4.0$ nm and $W_d = 0$. The structure in this case is, indeed, recovered to a semi-infinite SL attached to a semi-infinite homogeneous substrate c. The lower and higher shade areas are denoted as miniband 1 and 2, and the three regions from low to high separated by two allowed bands represent the first, second and third minigaps, respectively. Here, note that the first and third minigaps lie at the mini-Brillouin zone center, and the second minigap at the zone edge. The dotted curves are for the longitudinal energy spectra of the surface states lying in the corresponding minigaps. From Fig. 2, we can clearly observe the evolution of the surface states with the increase of the concentration y. Our calculated results showed that when $y < 0.3$, there exists only one surface state at the first minigap, and no surface states at the other minigaps (see Fig. 2(a)–(c)). With the increase of the concentration y, the surface state shifts towards the higher-energy region, and gradually merges into the bulk band from larger k_{xy} to smaller, finally vanishes when the concentration y is closed to 0.3, i.e., the barrier height of the substrate is nearly equal to that of the SL. When the potential of the substrate is larger than that of the barrier layer of the SL (i.e., $U_c > U_b$), a surface state begins to arise from the second minigap (see Fig. 2(d)). Moreover, it is also seen clearly that a surface state appears in the third minigap for certain k_{xy}. From the figure, we can find that the existence and the features of the surface states in different minigaps are dependent on the concentration y and the transverse wave number k_{xy}. Here, one may inquire if the conservation of total number of surface states in every minigap for every value of the wave number k_{xy} can be kept. We give physical explanations for this as follows: the formation of the bulk bands in SL results from the periodicity coupling between two adjacent layers, while for a SL with inhomogeneous layers such as surface or defect layers, the periodic coupling is locally broken down around the inhomogeneous layer of the SL. The periodicity-broken coupling will leads to the appearance of the new splitting levels. Some of them may lie within the bulk bands and develop into the delocalized scattering

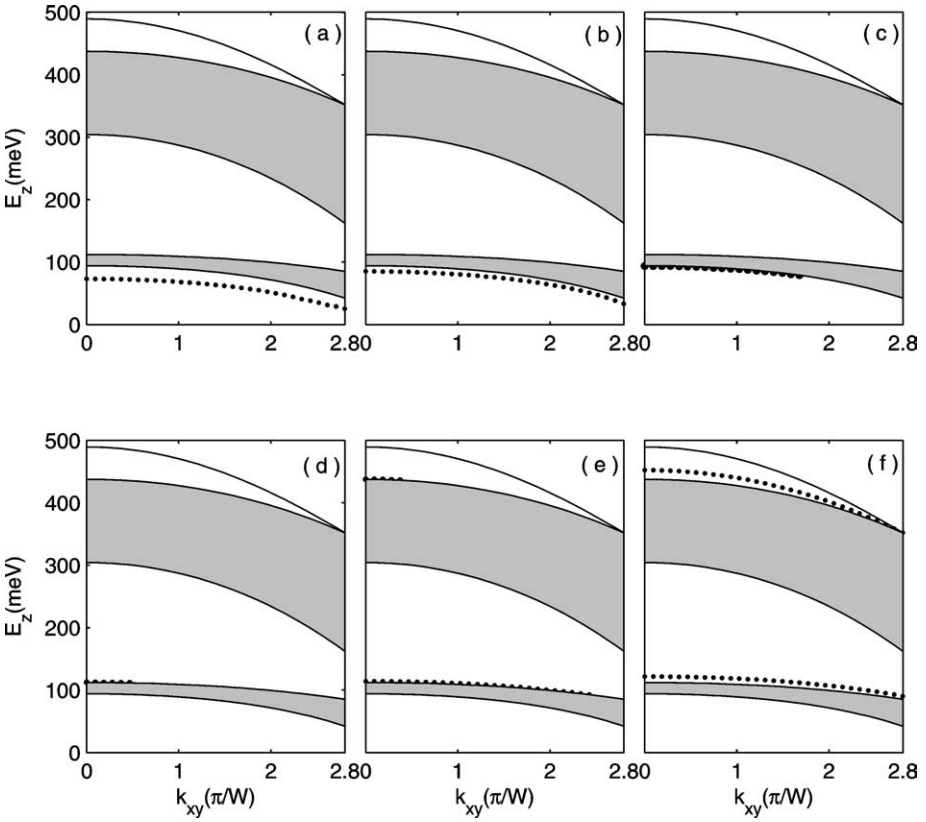

Fig. 2. Electronic energy spectra as a function of the transverse wave number k_{xy} for different concentration y of the semi-infinite homogeneous substrate. (a)–(f) correspond to $y = 0.1, 0.15, 0.23, 0.4, 0.5$ and 1.0, respectively. The lower and higher shade areas denote the scope of the first and second allowed minibands, respectively. The three regions from low to high separated by two minibands represent the first, second and third minigaps, respectively. The dotted curves denote the energy spectra of the surface states inside minigaps.

states, and the other part of them reside in the minigaps and become surface states located in the vicinity of the surface. Though the conservation of the total number of surface states is broken, the conservation of the total number of all splitting levels including both the delocalized scattering states and surface states is still kept for every value of the wave number k_{xy}. Fig. 2 also shows that with the increasing of the transverse wave number k_{xy} all minibands, minigaps and localized energy levels always monotonically shift towards lower-energy region, minibands become broader and the minigap more narrow, and the change of the higher-lying minibands and minigaps are faster than that of the lower ones. These results are attributed to the decrease of the effective-barrier height caused by the coupling effect as the transverse wave number k_{xy} increases (see Eq. (3)).

Fig. 3 gives the calculated electron longitudinal energy as a function of the potential height of the substrate for different k_{xy}: (a) for $k_{xy} = 0$ and (b) for $k_{xy} = 2.0(\pi/W)$. It is obvious that all minibands, minigaps and surface energy levels at $k_{xy} = 2.0(\pi/W)$ are lower than that at $k_{xy} = 0$, as is seen by comparing Fig. 3(a) and (b). To study the localized properties of the surface states at different transverse wave number k_{xy}, the modular square $|\phi|^2$ of the wave function of the surface states was calculated for $y = 0.15$ (i.e., $U_c = 141.6$ meV), which was used in the experimental observation of a surface state in superlattice [5], and is shown in Fig. 4. As expected, the wavefunction decays exponentially into the substrate and quickly into the semi-infinite SL. Clearly, the wave function is almost completely localized at the border of the substrate and the first well. This is why we name these

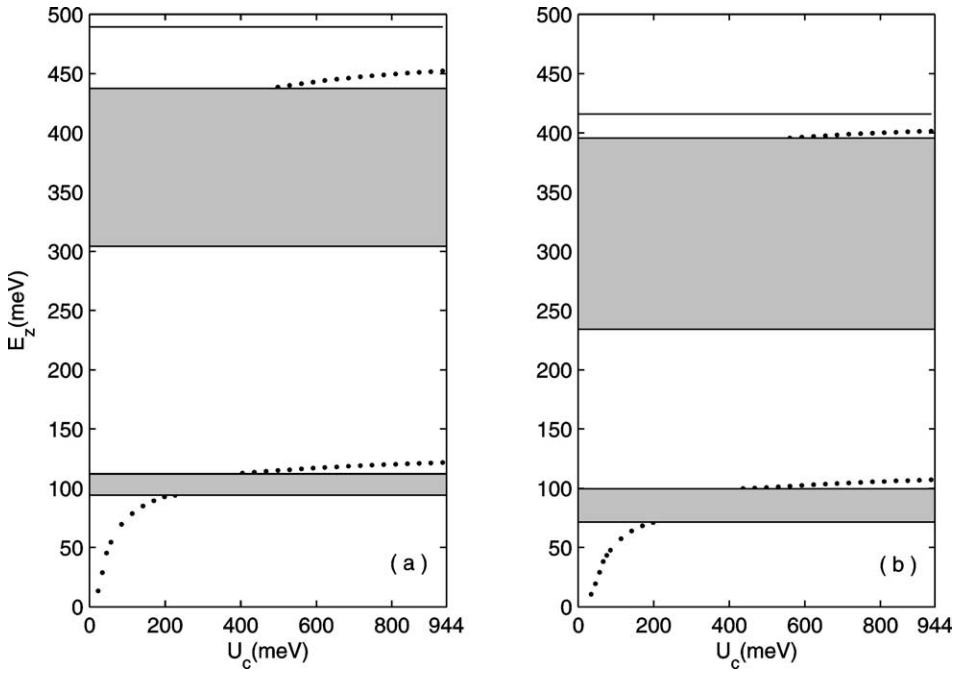

Fig. 3. Electronic energy spectra of the GaAs/$Al_{0.3}Ga_{0.7}As$ SL, terminated by a $Al_yGa_{1-y}As$ substrate c, as a function of the U_c, for different transverse wave number k_{xy}: (a) for $k_{xy} = 0$, (b) for $k_{xy} = 2.0(\pi/W)$. The dotted curves are the localized energy spectra lying in minigaps, respectively. Other parameters are the same as those in Fig. 2.

localized states as surface states. From Fig. 4, we can see clearly that when k_{xy} is smaller, its localization become stronger. This is due to the fact that when increasing the transverse wave number k_{xy}, the effect of coupling of the normal and lateral motion of an electron becomes bigger and the wavefunction of the electron penetrates further more into the substrate and SL, and thus the localization degree of the electron state become weaker.

In Fig. 5, we describe the dispersion curves of the longitudinal energy components of the surface states for the case where the concentration y of the semi-infinite homogeneous substrate c is fixed to unity (AlAs), and the concentration x of the cap layer d is varied from zero to unity: (a)–(f) correspond to $x = 0$, 0.2, 0.25, 0.27, 0.7 and 1.0, respectively. Here, we take $W_a = 4.0$ nm, $W_b = 4.0$ nm and $W_d = 3.0$ nm. When the $x < 0.3$ (i.e., $U_d < U_b$), only one localized state exists at the second and third minigap respectively. The localized electronic levels monotonically shift towards higher-energy region with an increase of x, and emerges into the minibands at $x = 0.3$. It is

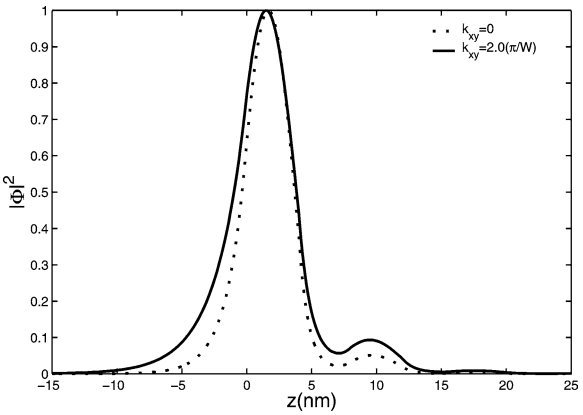

Fig. 4. The modular square $|\phi|^2$ of the wave functions of the surface states in the first minigap for different transverse wave number k_{xy}: the dotted curve for $k_{xy} = 0$, and the solid curve for $k_{xy} = 2.0(\pi/W)$, respectively.

interesting that the localized levels enter into the miniband from $2.8\pi/W$ to zero at the second minigap, while from zero to $2.8\pi/W$ in the third one. When $x > 0.3$, one localized state appears at the second and

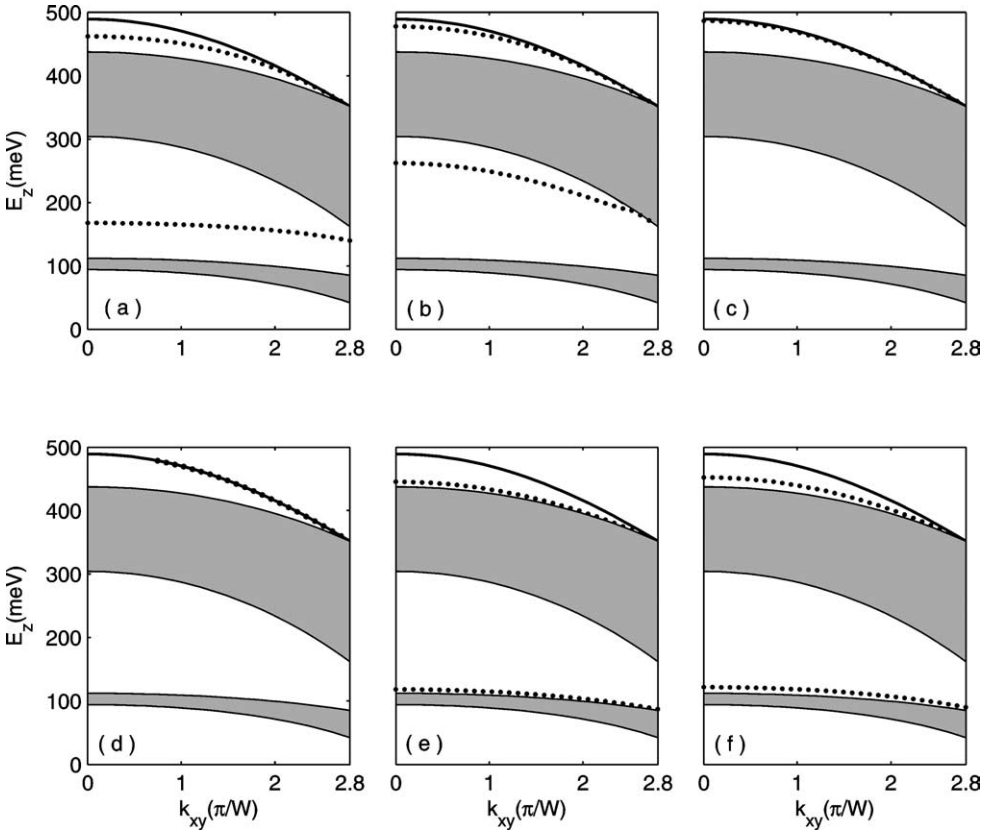

Fig. 5. Electronic energy spectra as a function of the transverse wave number k_{xy} for different concentration x of the cap layer. (a)–(g) correspond to $x = 0$, 0.2, 0.25, 0.27, 0.7 and 1.0, respectively. The dotted curves denote the energy spectra of the surface states inside minigaps. Others are the same as those in Fig. 2.

third minigap again, respectively, and monotonically shift towards higher-energy region with an increase of x. Fig. 5 clearly shows that all the localized states sensitively depend on the concentration x of the cap layer. The variation of the localized levels, minibands, and minigaps with the transverse wave number k_{xy} is similar to those in Fig. 2. If it is taken that the substrate potential U_c is larger than that of the SL barrier (namely $U_c < U_b$), similar features of the surface states can be obtained. However, the surface states only lie at the first minigap.

Fig. 6 describes the influence of the thickness W_d of the cap layer on the electronic level of the surface states for different k_{xy}: (a) for $k_{xy} = 0$ and (b) for $k_{xy} = 2.0(\pi/W)$. Here we take $x = 0.3$, and $y = 1.0$. In this case, we have $U_c > U_b$. As a consequence, the surface states have not been found at the first minigap. The surface states exist in the second or third minigaps only for some ranges of W_d. From Fig. 6 it is clearly observed that with the increase of W_d, the surface states monotonically decrease from upper miniband to the lower miniband. By comparing Fig. 6(a) with (b), we can find that the effect of the transverse wave number k_{xy} on minibands, minigaps and surface energy levels is obvious.

4. Summary

In this Letter, we have studied, for the first time to our knowledge, the coupling effect of the normal and lateral motions on the surface electron states in a semi-infinite SL with a cap layer and showed a detailed comparisons of surface electron levels between neglecting and including this coupling effect within the framework of the effective-mass theory. The ex-

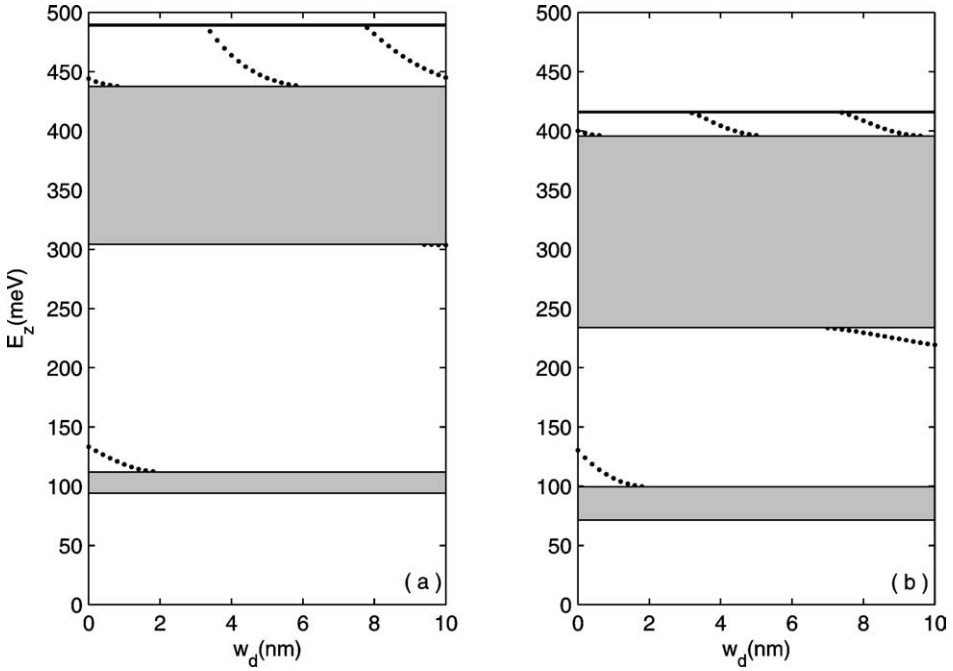

Fig. 6. Dependence of surface electron levels as a function of the width W_d of the cap layer at $U_c > U_b$ (the substrate is AlAs) for different transverse wave number k_{xy}: (a) for $k_{xy} = 0$, (b) for $k_{xy} = 2.0(\pi/W)$. The dotted curves denote the energy spectra of surface states inside minigaps. Others are the same as those in Fig. 2.

istence and properties of the surface electron states are sensitively dependent on the transverse number k_{xy}, and the concentration and thickness of the cap layer, as well as the concentration y of the $Al_yGa_{1-y}As$ substrate. It is found that with the increase of the transverse wave number k_{xy} minibands, minigaps and surface levels monotonously shift towards the lower-energy region, and minigaps become narrower and the minibands broader. Moreover, the coupling effect is more important on the higher-lying minibands, minigaps and surface electron states. In a word, the coupling effect between normal and lateral motions of an electron should be considered when the difference of the effective mass of the electron in the well and barrier layers cannot be neglected.

Acknowledgements

This work is supported by the National Science Foundation of China and the Ministry of Science and Technology of China 973 program (Project No. 2002CB613406).

References

[1] I. Tamm, Phys. Z. Sowjetunion 1 (1932) 733.
[2] M. Stęślicka, Prog. Surf. Sci. 50 (1995) 65.
[3] F. Agulló-Rueda, E.E. Mendez, H. Ohno, J.M. Hong, Phys. Rev. B 42 (1990) 1470.
[4] H. Ohno, E.E. Mendez, J.A. Brun, J.M. Hong, F. Agulló-Rueda, L.L. Chang, L. Esaki, Phys. Rev. Lett. 64 (1990) 2555.
[5] H. Ohno, E.E. Mendez, A. Alexandrou, J.M. Hong, Surf. Sci. 267 (1992) 161.
[6] R.H. Yu, Phys. Rev. B 47 (1993) 1379.
[7] D. Indjin, V. Milanović, Z. Ikonic, Phys. Rev. B 52 (1995) 16762.
[8] X.H. Wang, B.Y. Gu, G.Z. Yang, J. Wang, Phys. Rev. B 58 (1998) 4629.
[9] K.-Q. Chen, X.-H. Wang, B.-Y. Gu, Int. J. Mod. Phys. B 14 (2000) 2587.
[10] K.-Q. Chen, X.-H. Wang, B.-Y. Gu, Phys. Rev. B 61 (2000) 12075.
[11] S. Mizuno, Phys. Rev. B 65 (2002) 193302.

[12] K.-Q. Chen, X.-H. Wang, B.-Y. Gu, Phys. Rev. B 62 (2000) 9919.
[13] K.-Q. Chen, W. Duan, J. Wu, B.-L. Gu, B.-Y. Gu, J. Phys.: Condens. Matter 14 (2002) 13761;
K.-Q. Chen, W. Duan, J. Wu, B.-L. Gu, B.-Y. Gu, Phys. Lett. A 299 (2002) 634.
[14] R.C. Vilela, R.N. Costa, E.R. Nobre, V.N. Freire, E.L. Albuquerque, Phys. Rev. B 68 (2003) 033307.
[15] T. Miller, T.-C. Chiang, Phys. Rev. Lett. 68 (1992) 3339.
[16] P. Masri, L. Dobrzynski, B. Djafari-Rouhani, J.O.A. Idiodi, Surf. Sci. 166 (1986) 301.
[17] W.L. Bloss, Phys. Rev. B 44 (1991) 8035.
[18] F.Y. Huang, H. Morkoç, J. Appl. Phys. 71 (1992) 524.
[19] H.K. Sy, T.C. Chua, Phys. Rev. B 48 (1993) 7930.
[20] J. Arriage, F. Garcia-Moliner, V.R. Velasco, Prog. Surf. Sci. 42 (1993) 271.
[21] S. Fafard, Phys. Rev. B 50 (1994) 1961.
[22] E.H. Ei Boudouti, B. Djafari-Rouhani, A. Akjouj, L. Dobrzynski, R. Kucharczyk, M. Stęślicka, Phys. Rev. B 56 (1997) 9603.
[23] R. Kucharczyk, M. Stęślicka, B. Djafari-Rouhani, Phys. Rev. B 62 (2000) 4549.
[24] R. Kucharczyk, M. Stęślicka, B. Djafari-Rouhani, Surf. Sci. 482 (2001) 648.
[25] M. Hammouchi, A. Bousfia, E.H. Ei Boudouti, A. Nougaoui, B. Djafari-Rouhani, M.L.H. Lahlaouti, A. Akjouj, L. Dobrzynski, Moroccan J. Condens. Matter 1 (1999) 1.
[26] M. Stęślicka, R. Kucharczyk, A. Akjouj, B. Djafari-Rouhani, L. Dobrzynski, S.G. Davison, Surf. Sci. Rep. 47 (2002) 93.
[27] V.V. Paranjape, Phys. Rev. B 52 (1995) 10740.
[28] X.-H. Wang, B.-Y. Gu, G.Z. Yang, Phys. Rev. B 55 (1997) 9340.